

Gold–Ligand-Catalyzed Selective Hydrogenation of Alkynes into *cis*-Alkenes via H₂ Heterolytic Activation by Frustrated Lewis Pairs

Jhonatan L. Fiorio,[†] Núria López,[‡] and Liane M. Rossi^{*,†}

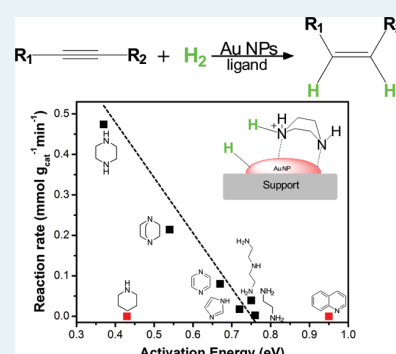
[†]Departamento de Química Fundamental, Instituto de Química, Universidade de São Paulo, Av. Prof. Lineu Prestes, 748, 05508-000 São Paulo, SP, Brazil

[‡]Institute of Chemical Research of Catalonia, ICIQ, The Barcelona Institute of Science and Technology, Av. Països Catalans 16, 43007 Tarragona, Spain

Supporting Information

ABSTRACT: The selective hydrogenation of alkynes to alkenes is an important synthetic process in the chemical industry. It is commonly accomplished using palladium catalysts that contain surface modifiers, such as lead and silver. Here we report that the adsorption of nitrogen-containing bases on gold nanoparticles results in a frustrated Lewis pair interface that activates H₂ heterolytically, allowing an unexpectedly high hydrogenation activity. The so-formed tight-ion pair can be selectively transferred to an alkyne, leading to a *cis* isomer; this behavior is controlled by electrostatic interactions. Activity correlates with H₂ dissociation energy, which depends on the basicity of the ligand and its reorganization on activation of hydrogen. High surface occupation and strong Au atom–ligand interactions might affect the accessibility and stability of the active site, making the activity prediction a multiparameter function. The promotional effect found for nitrogen-containing bases with two heteroatoms was mechanistically described as a strategy to boost gold activity.

KEYWORDS: gold, hydrogenation, alkyne, piperazine, frustrated Lewis pair



INTRODUCTION

Catalytic hydrogenation is a key process technology in the petrochemical industry and has evolved into an important transformation for the manufacture of pharmaceuticals and fine chemicals, replacing stoichiometric chemical reduction methods that generate large amounts of toxic waste. Catalytic hydrogenations are usually accomplished by the activation of molecular hydrogen via homolytic H₂ dissociation on metal surfaces, such as Rh, Pt, Pd, and Ni.^{1,2} Selective hydrogenations with discrimination between reducible functional groups, such as carbon–carbon triple and double bonds, are very challenging. Palladium remains the catalyst of choice for many hydrogenations, but the selective conversion of alkynes into *cis*-alkenes requires the use of a palladium catalyst partially poisoned with a metal such as lead (Lindlar catalysts).³ Auxiliary ligands containing N, S, and O groups have been combined with Pd and a secondary metal (Pb, V) to improve selectivity. The presence of toxic lead and catalyst deactivation are driving forces for the search of lead-free Lindlar catalyst replacements for alkyne to *cis*-alkene hydrogenations. More active and selective palladium catalysts have appeared, but there is still room for the development of catalyst systems based on alternative designs.^{4–6}

Gold nanoparticles (Au NPs) have attracted a significant amount of interest as catalysts, due to their exceptional selectivity and surprisingly high activity, which is not replicated by other metals, for reactions such as CO oxidation.^{7–10} In

comparison to the enormous number of studies with Au NP catalysts for oxidations, there are fewer studies in hydrogenations and gold was often considered only a modest hydrogenation catalyst.^{11–16} Ultrafine gold particles supported on alumina were regarded as a unique metal for the selective hydrogenation of acetylene into ethylene, and gold received attention as a selective catalyst for this gas-phase reaction.^{17,18} More recently, a new interest emerged in the selective hydrogenation of carbonyl or nitro groups.^{19–22} The main virtue was gold's unique chemoselectivity, which is controlled by the thermodynamics of the adsorption of the organic reactants and products.^{18,23} In general, the low activity associated with gold is a consequence of poor H₂ dissociation on gold,^{24,25} though nanostructuring can improve activity (H₂ dissociation) at structural defects on nanoparticles or nanoporous materials.¹⁸

The use of molecular modifiers or auxiliary ligands is a well-known strategy to enhance selectivity in heterogeneous catalysis, mainly as a result of ensemble control,^{26–28} and similarly capping ligands (e.g., nitrogen-containing bases) were found to influence the catalytic properties of metal nanoparticles.^{29–35} Quinoline is the most frequently used modifier, either by itself or with lead, for the selective hydrogenation of

alkynes performed on Pd Lindlar and Pt catalysts.^{36,37} Nitrogen-containing bases have also been explored as promoters for hydrogenation reactions by gold via H₂ activation (quinoline³⁸ and pyridine³⁹) and using other hydrogen sources, such as PhMe₂SiH⁴⁰ and HCOOH,⁴¹ in combination with reaction modifiers. The use of H₂ as the hydrogen source is highly desired, as it avoids the production of residues, but the channels for activation of H₂ on gold are not yet fully understood.

Herein, we report the unique promotion effect of nitrogen-containing bases on the catalytic activity of gold nanoparticles. The starting inactive gold nanoparticles supported on silica become highly active for the selective hydrogenation of alkyne into *cis*-alkenes. The hydrogenation proceeded smoothly and was fully selective using H₂ as the hydrogen source under relatively mild conditions (80 °C, 6 bar of H₂). According to density functional theory calculations, molecular hydrogen dissociation occurs at the ligand–gold interface, generating a tight-ion pair that can be selectively transferred to the adsorbed alkyne in a *cis* configuration controlled by electrostatic interactions.

■ EXPERIMENTAL SECTION

Materials and Methods. All reagents used for the support and catalyst preparation were of analytical grade, purchased from Sigma-Aldrich, and were used as received. Tetrachloroauric(III) acid was purchased as a 30 wt % aqueous solution in dilute HCl (Sigma-Aldrich). Alkynes, alkenes, amines, and standards for GC analysis were purchased from Sigma-Aldrich at the highest grade available and used as received. Liquid amines used as additives were purified by standard methods just before use. Ethanol (99.5%) and DMF (99%) were purchased from Synth (Brazil) and used as received. Toluene was purchased from Synth (Brazil) and dried before use. The glass reactor was thoroughly cleaned with aqua regia (HCl/HNO₃ 3/1 v/v), rinsed with copious amounts of pure water, and then dried in an oven prior to use. Gold content in the catalyst was measured by FAAS analysis, on a Shimadzu AA-6300 spectrophotometer using an Au hollow cathode lamp (Photron). Metal leaching into the supernatant solution was measured by ICP-AES, performed on a Spectro Arcos ICP AES instrument. UV–vis spectra were recorded on a Shimadzu UV-1700 instrument. TEM analyses were performed with a JEOL 2100 instrument. X-ray diffraction (XRD) of the samples was recorded using a Rigaku miniflex diffractometer with Cu K α radiation ($\lambda = 1.54 \text{ \AA}$) at a 2θ range from 20 to 90° with a 0.02° step size and measuring time of 5 s per step. GC analyses were carried out with a Shimadzu GC-2010 instrument equipped with a RTX-Wax column (30 m \times 0.25 mm \times 0.25 mm) and an FID detector. Method: $T_i = 40 \text{ }^\circ\text{C}$, $T_f = 200 \text{ }^\circ\text{C}$, 25 min, T FID, and SPLIT = 200 °C. Internal standard: biphenyl. The conversion and selectivity were determined from the total amount of detected products and reactant.⁴²

Preparation of Au/SiO₂ and Au/Fe₃O₄@SiO₂. Silica nanospheres (SiO₂) and silica-coated magnetite nanoparticles (Fe₃O₄@SiO₂) were obtained by means of a reverse micro-emulsion process and functionalized with (3-aminopropyl)-triethoxysilane, as reported elsewhere.⁴³ Gold nanoparticles were prepared by the impregnation–reduction method, as reported in the literature.⁴⁴ Typically, 1.0 g of the amino-modified support was added to 20 mL of HAuCl₄ aqueous solution ($1.3 \times 10^{-2} \text{ mol L}^{-1}$) with continuous stirring. After 30 min, the mixture was filtered and the solid thoroughly washed

with deionized water. The recovered material was dispersed in 10 mL of water, and an aqueous NaBH₄ solution (10 mL, 0.2 mol L⁻¹) was added dropwise with vigorous stirring. After further stirring for 20 min, the solid was recovered by filtration, thoroughly washed with water, and dried under vacuum. Both Au/SiO₂ and Au/Fe₃O₄@SiO₂ catalysts contain 3.4 wt % of gold as determined by FAAS.

Preparation of Au/Support (TiO₂, CeO₂, and Al₂O₃). Au NPs supported on TiO₂, CeO₂, and Al₂O₃ were prepared by the DP method, as reported in the literature.^{45,46} Typically, 1.0 g of oxide support was added to 100 mL of an aqueous solution of HAuCl₄ ($2.1 \times 10^{-3} \text{ mol L}^{-1}$) and urea (0.42 mol L⁻¹). The mixture was heated to 80 °C with vigorous stirring for 4 h, centrifuged, washed, and dispersed in 10 mL of water. Then, an aqueous NaBH₄ solution (10 mL, 0.2 mol L⁻¹) was added dropwise with vigorous stirring. After further stirring for 20 min, the solid was recovered by filtration, thoroughly washed with water, and dried under vacuum. The Au loadings were as follows: Au/TiO₂, 3.4 wt %; Au/CeO₂, 3.5 wt %, Au/Al₂O₃, 2 wt %.

General Procedure for Catalytic Hydrogenation of Alkynes. A typical procedure for the semihydrogenation of alkynes is as follows: alkyne (1 mmol), N-containing base (1 mmol), Au/SiO₂ (1 mol %), and 2 mL of solvent were placed in a modified Fischer–Porter 100 mL glass reactor. The reactor was purged five times with H₂, leaving the vessel at 6 bar. The resulting mixture was vigorously stirred using a Teflon-coated magnetic stirrer, and the temperature was maintained with an oil bath on a hot stirring plate connected to a digital controller (ETS-D5 IKA). After the desired time, the catalyst was removed by centrifugation and the products were analyzed by GC with an internal standard to determine the conversion of alkyne and the selectivity for alkene. For kinetic studies, the reaction was performed using 4 times the amount of each component given above and aliquots were collected and analyzed by GC at different reaction time intervals. To determine the isolated yield of the obtained products, after the reaction was complete, the crude reaction mixture was transferred to a extraction funnel and treated with HCl (20 mL, 10% v/v). The aqueous phase was extracted three times with 5 mL of dichloromethane. The organic layers were dried with anhydrous MgSO₄, and the solvent was removed under reduced pressure, to give the corresponding desired alkene. ¹H NMR confirmed the purity of the isolated products. Details on other catalyst tests (catalyst recycling, scale-up, isotope H₂–D₂ exchange, isotopic effect) are given in the [Supporting Information](#).

Computational Details. Density functional theory calculations were performed on slabs representing the gold surface with the VASP code.^{47,48} The RPBE was the functional of choice,⁴⁹ and due to the large size of the molecules dispersion terms were introduced through our modified version of the D2 formulation⁵⁰ for the metal. The inner electrons were replaced by PAW,⁵¹ and the valence electrons were expanded in plane waves with a kinetic cutoff energy of 450 eV. The Au(111) surface was represented by a p(4 \times 4) supercell and four metal layers (>12 Å vacuum) for the adsorption and reaction. The *k*-point sampling was 3 \times 3 \times 1 in the Monkhorst–Pack scheme.⁵² Transition states were located through the climbing image nudged elastic band (ci-NEB) method;⁵³ the nature of the structures was assessed through the vibrational analysis with a 0.02 Å step.

RESULTS AND DISCUSSION

Screening of a series of N-containing bases (**B1**–**B19**) (see [Table S1](#) in the Supporting Information) with a broad range of pK_a values and chemical structures (primary, secondary, and tertiary amines and also heteroaromatic and cycloaliphatic amines) for the hydrogenation of phenylacetylene **1a** over Au NPs supported on silica (Au/SiO₂) with an average diameter of 2.3 ± 0.6 nm (see [Figure S1](#) in the Supporting Information), provided the results shown in [Figure 1](#).

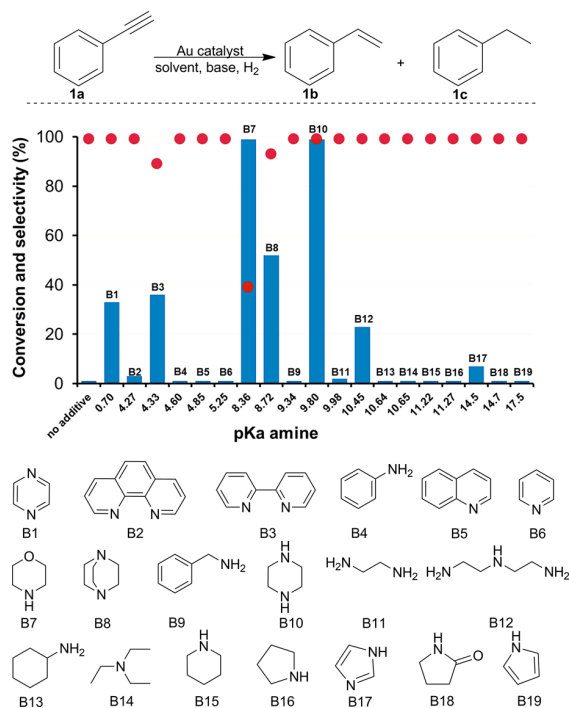


Figure 1. Screening of nitrogen-containing bases for phenylacetylene (**1a**) hydrogenation with Au/SiO₂ catalyst. Reaction conditions: 1 mmol of **1a**, 0.01 mmol of Au (50 mg of Au/SiO₂), 1 mmol of amine, 2 mL of ethanol, 100 °C, 6 bar of H₂, 24 h.

Au/SiO₂ itself performed poorly (conversion <1%), but it is highly selective and provides exclusively the alkene **1b**. The Au/SiO₂ catalyst becomes active in the presence of some of the N-containing bases studied, but there was no correlation with the amine pK_a values. In general, nitrogen-containing bases with two heteroatoms (pyrazine (**B1**), 2,2-bipyridine (**B3**), morpholine (**B7**), 1,4-diazabicyclo[2.2.2]octane (DABCO; **B8**), piperazine (**B10**), and imidazole (**B17**)) exhibited a higher promotion effect in the hydrogenation of **1a** by gold than species with one nitrogen atom. Morpholine (**B7**) was able to give full conversion of **1a**, but a competing hydroamination process³⁹ occurred and the ketone product was formed in the crude products (selectivity for acetophenone **1d**: 60%). Piperazine (**B10**) provided full conversion of **1a** and 100% selectivity to the alkene **1b**, giving the best catalytic result among the amines tested. It is worth mentioning that a blank experiment with **B10** and without the catalyst or with the support without Au NPs showed no conversion of **1a** ([Table S2](#) in the Supporting Information). Another experiment carried out in the presence of catalyst but in the absence of H₂ (reaction performed under a nitrogen atmosphere) showed no conversion of **1a** ([Table S2](#)). A filtration test revealed that the

obtained activity is not related to any leaching of the catalytically active metal (no remaining activity in the supernatant), which suggests that gold surfaces containing adsorbed auxiliary ligands catalyze the hydrogenation reaction. In order to further examine the stability of the Au NP catalyst upon recycles, a magnetic version of the silica support was synthesized to avoid any mass loss during the recycles. The magnetic catalyst (Au/Fe₃O₄@SiO₂) was easily recovered by magnetic separation, and the recovered solid remains active for five successive reactions using fresh portions of **1a**, piperazine (**B10**), and solvent ([Figure S2](#) in the Supporting Information). ICP AES analysis of the liquid products isolated after magnetic separation showed negligible amounts of gold (detection limit: 0.10 ppm). These results corroborate the filtration test, suggesting that the catalytically active metal remains at the support and does not leach into the solution.

The Au/SiO₂ catalyst was further tested in the hydrogenation of **1a** using different solvents and temperatures. The “green” and protic solvent ethanol gave the best catalytic results (full conversion), while aprotic solvents such as toluene and DMF were slightly less efficient ([Table S2](#) in the Supporting Information). Decreasing the reaction temperature to 80 °C did not affect the conversion and selectivity, while further reduction of the temperature to 60 °C caused a decrease in conversion to 53% ([Table S2](#)). On the basis of the above experiments, we chose ethanol as solvent, piperazine (**B10**) as the auxiliary ligand, and a temperature of 80 °C as the optimized conditions for the semihydrogenation reaction. We further examined Au NPs immobilized on different supports, such as Au/Al₂O₃, Au/TiO₂, and Au/CeO₂, under the aforementioned conditions ([Table S2](#)). TiO₂ provided the same activity and selectivity as for SiO₂, but the CeO₂ support was detrimental to activity while the Al₂O₃ support was detrimental to selectivity. Next, we turned our attention to analyze the effect of adding different amounts of piperazine (**B10**) ([Figure 2](#)). A very low conversion of **1a** (13%) was obtained using 1a:ligand:Au 100:1:1 ([Figure 2a](#)), but full

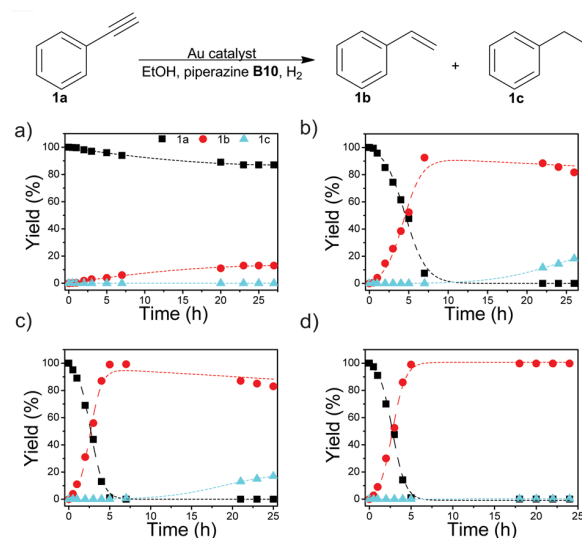


Figure 2. Time course of hydrogenation of phenylacetylene catalyzed by Au/SiO₂ with increasing amounts of piperazine: (a) 0.04 mmol; (b) 0.4 mmol; (c) 2 mmol; (d) 4 mmol. Reaction conditions: 4 mmol of phenylacetylene, 0.04 mmol of Au, 0.04–4 mmol of amine, 8 mL of ethanol, 80 °C, 6 bar of H₂.

Table 1. Scope of Semihydrogenation of Alkynes to Alkenes Using Au/SiO₂ and Piperazine B10^a

$$R_1-C\equiv C-R_2 \xrightarrow[\text{EtOH, piperazine B10, H}_2]{\text{Au catalyst}} \begin{matrix} R_1 & R_2 \\ \diagdown & / \\ C & = & C \\ / & \diagdown \\ H & & H \end{matrix}$$

Entry	Substrate	t (h)	Conv. (%) ^b	Selectivity (%) ^b	Z:E ^c	Entry	Substrate	t (h)	Conv. (%) ^b	Selectivity (%) ^b	Z:E ^c
1		5	>99	>99	-	13		24	>99	>99	-
2	1a + 1b (1:1)	24	>99	>99	-	14		15	>99	>99	-
3 ^d	1a + 1b (1:100)	24	>99	99	-	15 ^e		24	35	>99	-
4		17	>99	>99	-	16		16	34	>99	-
5		23	>99	>99	-	17		22	>99	79	-
6 ^e		45	43	>99	-	18		24	>99	94	-
7		12	>99	>99	-	19		24	>99	99	-
8		22	>99	>99	-	20		6	99 (80%)	>99	97:3
9		24	>99	>99	-	21		24	>99 (79%)	>99	100:0
10		24	>99	>99	-	22		24	60	>99	100:0
11 ^f		45	91 (84%)	>99	-	23		24	89 (75%)	>99	100:0
12		24	>99	>99	-	24		24	>99	>99	100:0
						25		24	90	>99	100:0

^aReaction conditions unless specified otherwise: 1 mmol of alkyne, 0.01 mmol of Au, and 1 mmol of piperazine (**B10**), in 2 mL of ethanol at 80 °C and 6 bar of H₂. ^bDetermined by GC using internal standard techniques (>99% denotes that no other product was detected); values in parentheses refer to isolated yields. ^cZ/E ratio was determined by ¹H NMR spectroscopy. ^d1% of alkane detected by GC. ^e0.02 mmol of Au and toluene as solvent (2 mL). ^f0.02 mmol of Au. ^gToluene as solvent (2 mL).

conversion was achieved with any other concentration of **B10** studied (Figure 2b–d). The hydrogenation of styrene (**1b**) to ethylbenzene (**1c**) was completely suppressed when a large excess of **B10** was used (**1a**:ligand: Au 100:100:1). It is worth noting that the reaction rate is enhanced with an increase in the concentration of the piperazine (reaction rates 0.87, 9.0, 15.7, and 15.4 mmol g_{cat}⁻¹ h⁻¹, for 1, 10, 50, and 100 equiv of **B10**, respectively), suggesting that not only does piperazine play a very important role in the activation of Au NPs as hydrogenation catalysts (activity enhancement effect) but it also works as a selectivity enhancer to avoid the subsequent hydrogenation of the alkene into alkane. Particularly, in large excess of piperazine (**1a**:ligand: Au 100:100:1), which would correspond to about 240 ligands per surface Au atom (estimated surface atoms 42%), the alkene desorbs without being converted into the alkane.

Due to the high selectivity of the Au/SiO₂:piperazine (1:100 Au:**B10**) catalytic system for the conversion of phenylacetylene (**1a**) into styrene (**1b**) (Table 1, entry 1), it was tested in a competition hydrogenation experiment starting from a mixture of phenylacetylene (**1a**) and styrene (**1b**) (Table 1, entries 2 and 3). These experiments revealed that the reaction selectivity is maintained even in large excess of the alkene **1b** and are relevant to evaluate the application of our gold catalyst system for the purification of styrene, which is an important monomer and usually contains small quantities of acetylenic compounds, which poison olefin polymerization catalysts and must be removed via selective hydrogenation before polymerization.⁵⁴ Under competitive conditions, Au/SiO₂ catalyst converted preferentially the alkyne **1a** to alkene **1b** and less than 1% of ethylbenzene **1c** was formed.

Finally, the general applicability and limitation of the methodology was evaluated through the hydrogenation of

alkynes under the optimized conditions (100:1:100 alkyne: Au: **B10**). A variety of terminal and internal alkynes were readily hydrogenated to the desired alkene and *cis*-alkene with moderate to excellent yield with, importantly, hardly any over-reduction to alkane (Table 1). Moreover, both electron-deficient substituents, such as esters (Table 1, entry 25), and electron-rich groups, for example amino and methoxy (Table 1, entries 15 and 16), were tolerated well. Clearly, the most challenging substrates are alkynes with an alkene moiety (Table 1, entries 6, 11, and 19). We were pleased that our Au NP catalyst system was able to reduce only the alkyne unit without any detectable concurrent reduction of the alkene moieties in both the parent and product molecules. The results depicted in Table 1 confirmed that a broad range of sensitive and reducible functional groups, including halide, ether, and ester substituents (Table 1, entries 12–16 and 25), were tolerated in the alkyne hydrogenation process. The prominent isoprene, which is an essential building block in the polymer industry, was obtained via hydrogenation of 2-methylbut-1-en-3-yne (**9a**) (Table 1, entry 11) in 84% isolated yield. (*Z*)-Alkenes were mostly formed from internal alkynes (Table 1, entries 20–25). Notably, the semihydrogenation of nonpolar internal alkynes such as diphenylacetylene (**18a**) (Table 1, entry 20) and 1-phenyl-1-propyne (**19a**) (Table 1, entry 21) proceed quite smoothly under mild conditions. The only functional groups that do not tolerate the reaction conditions are aldehydes, ketones, and carboxylic acids (Table S3 in the Supporting Information), which are known to couple with amines. The catalyst system was also applicable for scaled-up conditions; **1a** (50 mmol, 5.1 g) and **18a** (50 mmol, 8.9 g) were successfully converted into the alkenes **1b** (4.6 g, 88%) and **19b** (7.1 g, 79%), respectively. Considering full conversion, a turnover number (TON) of 5000 was reached, with an excellent productivity of approximately 200 mol mol⁻¹ h⁻¹. These TON and productivity values (not optimized) are remarkably higher than those reported for other heterogeneous Au catalyst systems for semihydrogenation of alkynes employing molecular hydrogen or any other hydrogen source.^{39,55–58}

On the basis of the aforementioned facts and bearing in mind that primary and secondary amines are used as ligands in homogeneous catalysis to promote heterolytic cleavage of H₂ to give metal hydride species,^{38,34} we suggest that the key role of piperazine (**B10**) is to facilitate the crucial heterolytic H₂ activation at the Au NPs. Namely, the nitrogen atom of **B10** can serve as a basic ligand to promote the heterolytic H₂ cleavage, providing a favorable situation for hydrogen activation under very mild conditions. The reaction network and the configurations are presented in Figure 3. Piperazine (**B10**) is adsorbed on the gold surface through one of the N centers; due to the configuration in a boat site the second N is higher on the surface. The adsorption energy is sufficiently low (−0.27 eV) to ensure that no leaching of gold occurs.⁵⁹ Upon adsorption, the H₂ molecule can split between the ligand, forming a quaternary N center and a second H that goes to the surface. Such heterolytic splitting has been proposed for phosphine ligands,^{60–63} nitrogen ligands on metals,⁶⁴ and single-atom catalysts,^{3,65} while the active participation of the reactant in the activation of H₂ was also found for Ag catalysts in hydrogenation.⁶⁶ The metal–ligand system can be understood as a tight ion pair induced by the frustrated Lewis pair (FLP) formed by the ligand and the surface.^{67,68} H₂ dissociation occurs on the Au(111) surface through an energy barrier of 1.45 eV; the reaction is endothermic by 0.69 eV. Instead, if the

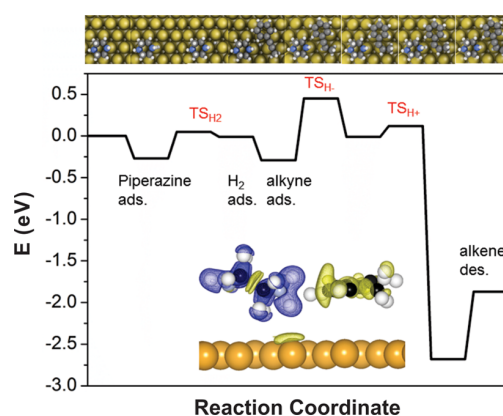


Figure 3. Reaction energy profiles with the corresponding configurations for the hydrogenation of 1-phenyl-1-propyne (**19a**). The inset corresponds to the charge distribution with respect to the neutral fragments after the first hydrogenation step. The separation between the yellow and blue colors indicates the electrostatic interactions. Yellow spheres represent Au, blue N, black C, and white H.

surface is decorated with piperazine (**B10**) the dissociation shows a barrier of 0.32 eV (therefore close to 0 if zero-point vibrational energies, ZPVE, are taken into account) and the final state is thermoneutral in comparison to the reactants (H₂ and the FLP). Then the alkyne can be adsorbed on the Au(111). Alkynes are weakly adsorbed on Au, but due to the van der Waals contributions the adsorption energy is −0.28 eV for 1-phenyl-1-propyne (**19a**). From the coadsorbed state, the hydride can be transferred to the alkyne. The reaction is slightly endothermic by 0.28 eV, the barrier being 0.74 eV from the coadsorbed state. Upon the first hydrogenation the moiety is negatively charged and interacts by electrostatic forces with the protonated piperazine (**B10**); this is shown in the inset of Figure 3. From this pair, proton transfer occurs, with a barrier of 0.13 eV, and the total process is exothermic by −2.39 eV. The alkene requires 0.53 eV for desorption. The particular structures for the transition states are shown in Figure 4. Note

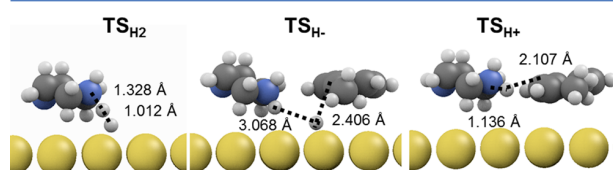


Figure 4. Transition state geometries for the hydrogenation of 1-phenyl-1-propyne (**19a**). Yellow spheres represent Au, blue N, black C, and white H.

that even if H₂ is barrierless according to the potential energy surface the introduction of entropies in the gas phase molecules implies that there is an entropic barrier on going from the gas to the adsorbed phase.⁶⁹ Finally, an alternative path considering first the transfer of the H⁺ and then the hydride was calculated; however, the intermediate is more than 1.5 eV higher in energy than that of the H⁻, H⁺ transfer and thus was discarded.

Calculations also highlight the limited basicity window for the N-containing bases able to provide the aforementioned promotion effect for hydrogenation on gold surfaces. Piperazine (**B10**) is unique because it is not strongly bound to the surface, and thus cannot extract the metal, for instance in comparison to

pyridine (**B6**). The binding energies for the linear complexes from the atomic reference are exothermic for pyridine (**B6**) (-0.1 eV) and very endothermic for piperazine (**B10**) (>5 eV). On comparison of the N-containing bases (Figure 5), the

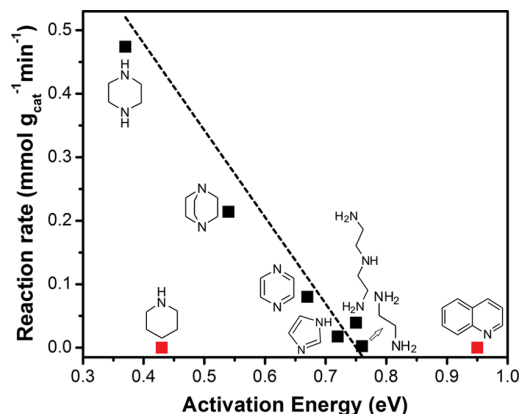


Figure 5. Reaction rates (experimental) as a function of the computed activation energies for heterolytic H_2 dissociation at the N ligand–Au(111) interface (without zero-point correction). The fitting shows that the activity is completely dominated by the H_2 activation. The red points stand for the molecules containing ligands with single N donors. As shown here they do not belong to the same family: for quinoline the adsorption is too strong, blocking the reactants on the surface, while for piperidine the ligand cannot compete with the reactant for adsorption and thus cannot effectively activate H_2 .

activity (reaction rates were obtained from the kinetic curves given in Figure S3 in the Supporting Information) is found to correlate with the energy barrier for H_2 dissociation at the ligand/Au(111) interface for piperazine, DABCO, pyrazine, imidazole, ethyleneamine, and diethylenetriamine (Table S4 in the Supporting Information). The barrier is the lowest for **B10**, thus indicating the unique catalytic activity of the piperazine–gold interface. The barrier for the activation is formed by different terms. One stems from the formation of a proton–hydride pair, this is a constant going from H_2 to a $\text{H}^+\cdots\text{H}^-$ pair separated by an average distance of 2 Å. The second appears as a consequence of the intrinsic basicity of the N-containing bases. A third term appears since at the transition state some of the N-containing bases need to rearrange in order to be an active part in the transition state; this is the case for quinoline (**B5**), which presents a much larger H_2 splitting barrier than would correspond to its thermodynamic (ΔE) value. The fourth term depends on the adsorption of H^- to the metal, which is in this case invariant. Notice that **B5** due to its large size can also block too many adsorption sites. Finally, the structures with two basic N heteroatoms seem to be more active for hydrogenation purposes. There are two reasons for this: the first is that two molecules can be dissociated for each ligand, thus being doubly active. This is clear with imidazole (**B17**), as only one of the N atoms seems capable of trapping H_2 (note that diethylenetriamine (**B12**) converts 23% while imidazole (**B17**) about 7% even if the barriers are comparable). The second reason is that having only one N heteroatom does not ensure adsorption to the surface for systems, such as piperidine (**B15**), which contains only one N. Piperidine (**B15**) thus easily leaves the surface, as in the transition state structure there is no element binding it to the surface, making the configuration unstable.

Finally, to gain a better understanding of the H_2 activation process, we conducted H_2 – D_2 exchange experiments (Au catalyst, toluene, H_2 : D_2 1:1, 6 bar, 80 °C, 24 h). The H_2 – D_2 exchange, attested by the formation of HD in the gas phase (detected by mass spectrometry m/z 3), was much higher over the Au/**B10** systems than that with pure Au catalyst. These results suggest that H_2 and D_2 molecules dissociate and recombine to produce HD, and this process is significantly enhanced by piperazine. When H_2 was switched for D_2 in the hydrogenation reaction under similar conditions, it was noteworthy that a primary isotope effect ($k_{\text{H}}/k_{\text{D}} \approx 2.7$, Figure S4 in the Supporting Information) was observed, suggesting that hydrogen is involved in the rate-determining step.⁷⁰ To obtain quantitative information about H_2 dissociation, different amounts of **1a** were hydrogenated under limited H_2 conditions (H_2 was preadsorbed on Au/ SiO_2 catalyst and the **B10**/Au/ SiO_2 catalyst system and the reaction was conducted under an inert atmosphere; see details in the Supporting Information and Table S5). Within the limits of experimental error, when **1a** was increased from 0.01 to 0.05 mmol, a similar amount of **1b** (~ 0.008 mmol) was obtained, allowing us to estimate that **H2** was the limiting reagent (~ 0.008 mmol of H_2 activated by **B10**/Au catalyst). For pure Au catalyst, a low yield of **1b** (~ 0.0001 – 0.00045 mmol) was obtained, confirming the very unfavorable hydrogen dissociation by Au in the absence of **B10**.

On the basis of the experimental and theoretical results described above, we propose the mechanism shown in Figure 6 for the hydrogenation of alkynes by Au NPs, which is possible in the presence of adsorbed piperazine due to the heterolytic activation of H_2 via frustrated Lewis pairs.

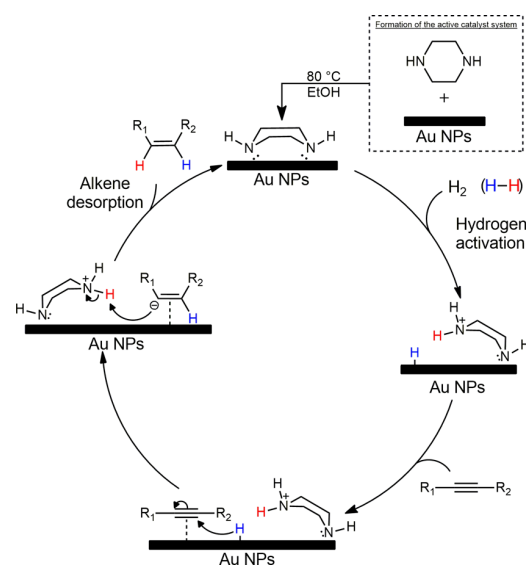


Figure 6. Proposed mechanism for gold-catalyzed catalytic hydrogenation of alkynes into *cis*-alkenes via a frustrated Lewis pair approach.

CONCLUSIONS

In summary, we have described that high conversion of a range of alkynes with excellent selectivity for *cis*-alkenes was achieved by combining supported Au NPs, N-containing bases, and H_2 as hydrogen source. We emphasize the role of the nitrogen-containing ligand as a means for substantial enhancement of

catalytic activity and selectivity, since the auxiliary ligands play a key role by opening a new channel for the heterolytic dissociation of molecular hydrogen on the frustrated Lewis pair. This ability to switch on the catalytic activity of Au NPs provides a promising new method for controlling a reactive system with ligands. The control is such that stereochemistry of the addition is also achieved due to electrostatic forces. A delicate balance among (i) the basicity of the ligand, (ii) the reorganization energy of the ligand to activate H₂, (iii) the possibility of site blocking by large ligands, and (iv) the metal leaching induced by some ligands is responsible for the activity–selectivity–stability controls in the catalyst system. We believe this remarkable promotional effect by N-containing ligands may have implications for gold catalysis while stimulating more applications in the field of selective hydrogenations not envisaged before. The versatile concept presented can be transferable to other metal nanoparticle catalysts.

■ ASSOCIATED CONTENT

📄 Supporting Information

Additional experimental results and details, characterization of catalysts, procedures, and characterization data, including NMR spectra (PDF)

■ AUTHOR INFORMATION

Corresponding Author

*E-mail for L.M.R.: lrossi@iq.usp.br.

ORCID

Jhonatan L. Fiorio: 0000-0001-7435-7430

Núria López: 0000-0001-9150-5941

Liane M. Rossi: 0000-0001-7679-0852

Notes

The authors declare no competing financial interest.

■ ACKNOWLEDGMENTS

The authors are grateful to the INCT-Catalise and the Brazilian government agencies FAPESP (Grant 2016/167387), CNPq, and CAPES for financial support. N.L. thanks the BSC-RES for providing generous computational resources.

■ REFERENCES

- (1) Kyriakou, G.; Boucher, M. B.; Jewell, A. D.; Lewis, E. A.; Lawton, T. J.; Baber, A. E.; Tierney, H. L.; Flytzani-Stephanopoulos, M.; Sykes, E. C. H. *Science* **2012**, *335*, 1209–1212.
- (2) Vilé, G.; Albani, D.; Almora-Barrios, N.; López, N.; Pérez-Ramírez, J. *ChemCatChem* **2016**, *8*, 21–33.
- (3) Vilé, G.; Albani, D.; Nachttegaal, M.; Chen, Z.; Dontsova, D.; Antonietti, M.; López, N.; Pérez-Ramírez, J. *Angew. Chem., Int. Ed.* **2015**, *54*, 11265–11269.
- (4) Jagadeesh, R. V.; Surkus, A.-E.; Junge, H.; Pohl, M.-M.; Radnik, J.; Rabeah, J.; Huan, H.; Schunemann, V.; Bruckner, A.; Beller, M. *Science* **2013**, *342*, 1073–1076.
- (5) Westerhaus, F. A.; Jagadeesh, R. V.; Wienhöfer, G.; Pohl, M.-M.; Radnik, J.; Surkus, A.-E.; Rabeah, J.; Junge, K.; Junge, H.; Nielsen, M.; Brückner, A.; Beller, M. *Nat. Chem.* **2013**, *5*, 537–543.
- (6) Chen, F.; Kreyenschulte, C.; Radnik, J.; Lund, H.; Surkus, A.; Junge, K.; Beller, M. *ACS Catal.* **2017**, *7*, 1526–1532.
- (7) Hashmi, A. S. K.; Hutchings, G. J. *Angew. Chem., Int. Ed.* **2006**, *45*, 7896–7936.
- (8) Ciriminna, R.; Falletta, E.; Della Pina, C.; Teles, J. H.; Pagliaro, M. *Angew. Chem., Int. Ed.* **2016**, *55*, 14210–14217.
- (9) Wittstock, A.; Bäumer, M. *Acc. Chem. Res.* **2014**, *47*, 731–739.
- (10) Stratakis, M.; Garcia, H. *Chem. Rev.* **2012**, *112*, 4469–4506.
- (11) Bond, G. C.; Sermon, P. A. *J. Chem. Soc., Chem. Commun.* **1973**, 444b–445b.
- (12) Bond, G. *Gold Bull.* **2008**, *41*, 235–241.
- (13) Cárdenas-Lizana, F.; Keane, M. A. *J. Mater. Sci.* **2013**, *48*, 543–564.
- (14) Wang, X.; Cárdenas-Lizana, F.; Keane, M. A. *ACS Sustainable Chem. Eng.* **2014**, *2*, 2781–2789.
- (15) García-Mota, M.; Cabello, N.; Maseras, F.; Echavarren, A. M.; Pérez-Ramírez, J.; Lopez, N. *ChemPhysChem* **2008**, *9*, 1624–1629.
- (16) Zhang, Y.; Cui, X.; Shi, F.; Deng, Y. *Chem. Rev.* **2012**, *112*, 2467–2505.
- (17) Jia, J.; Haraki, K.; Kondo, J. N.; Domen, K.; Tamaru, K. *J. Phys. Chem. B* **2000**, *104*, 11153–11156.
- (18) Segura, Y.; López, N.; Pérez-Ramírez, J. *J. Catal.* **2007**, *247*, 383–386.
- (19) Grrirane, A.; Corma, A.; García, H. *Science* **2008**, *322*, 1661–1664.
- (20) Corma, A.; Serna, P.; García, H. *J. Am. Chem. Soc.* **2007**, *129*, 6358–6359.
- (21) Claus, P.; Brücker, A.; Mohr, C.; Hofmeister, H. *J. Am. Chem. Soc.* **2000**, *122*, 11430–11439.
- (22) Corma, A.; Serna, P. *Science* **2006**, *313*, 332–334.
- (23) Vilé, G.; Albani, D.; Almora-Barrios, N.; López, N.; Pérez-Ramírez, J. *ChemCatChem* **2016**, *8*, 21–33.
- (24) Hammer, B.; Norskov, J. K. *Nature* **1995**, *376*, 238–240.
- (25) Fujitani, T.; Nakamura, I.; Akita, T.; Okumura, M.; Haruta, M. *Angew. Chem., Int. Ed.* **2009**, *48*, 9515–9518.
- (26) Mallat, T.; Baiker, A. *Appl. Catal., A* **2000**, *200*, 3–22.
- (27) Schoenbaum, C. A.; Schwartz, D. K.; Medlin, J. W. *Acc. Chem. Res.* **2014**, *47*, 1438–1445.
- (28) Giesbrecht, P. K.; Herbert, D. E. *ACS Energy Lett.* **2017**, *2*, 549–555.
- (29) Marshall, S. T.; O'Brien, M.; Oetter, B.; Corpuz, A.; Richards, R. M.; Schwartz, D. K.; Medlin, J. W. *Nat. Mater.* **2010**, *9*, 853–858.
- (30) Chen, G.; Xu, C.; Huang, X.; Ye, J.; Gu, L.; Li, G.; Tang, Z.; Wu, B.; Yang, H.; Zhao, Z.; Zhou, Z.; Fu, G.; Zheng, N. *Nat. Mater.* **2016**, *15*, 564–569.
- (31) Kwon, S. G.; Krylova, G.; Sumer, A.; Schwartz, M. M.; Bunel, E. E.; Marshall, C. L.; Chattopadhyay, S.; Lee, B.; Jellinek, J.; Shevchenko, E. V. *Nano Lett.* **2012**, *12*, 5382–5388.
- (32) Moreno, M.; Ibañez, F. J.; Jasinski, J. B.; Zamborini, F. P. *J. Am. Chem. Soc.* **2011**, *133*, 4389–4397.
- (33) Wu, B.; Huang, H.; Yang, J.; Zheng, N.; Fu, G. *Angew. Chem., Int. Ed.* **2012**, *51*, 3440–3443.
- (34) Schrader, L.; Warneke, J.; Backenköhler, J.; Kunz, S. *J. Am. Chem. Soc.* **2015**, *137*, 905–912.
- (35) Kahsar, K. R.; Schwartz, D. K.; Medlin, J. W. *J. Am. Chem. Soc.* **2014**, *136*, 520–526.
- (36) Chinchilla, R.; Nájera, C. *Chem. Rev.* **2014**, *114*, 1783–1826.
- (37) García-Mota, M.; Gómez-Díaz, J.; Novell-Leruth, G.; Vargas-Fuentes, C.; Bellarosa, L.; Bridier, B.; Pérez-Ramírez, J.; López, N. *Theor. Chem. Acc.* **2011**, *128*, 663–673.
- (38) Ren, D.; He, L.; Yu, L.; Ding, R. S.; Liu, Y. M.; Cao, Y.; He, H. Y.; Fan, K. N. *J. Am. Chem. Soc.* **2012**, *134*, 17592–17598.
- (39) Li, G.; Jin, R. *J. Am. Chem. Soc.* **2014**, *136*, 11347–11354.
- (40) Yan, M.; Jin, T.; Ishikawa, Y.; Minato, T.; Fujita, T.; Chen, L.-Y.; Bao, M.; Asao, N.; Chen, M.-W.; Yamamoto, Y. *J. Am. Chem. Soc.* **2012**, *134*, 17536–17542.
- (41) Li, S.-S.; Tao, L.; Wang, F.-Z.-R.; Liu, Y.-M.; Cao, Y. *Adv. Synth. Catal.* **2016**, *358*, 1410–1416.
- (42) Scanlon, J. T.; Willis, D. E. *J. Chromatogr. Sci.* **1985**, *23*, 333–340.
- (43) Jacinto, M. J.; Kiyohara, P. K.; Masunaga, S. H.; Jardim, R. F.; Rossi, L. M. *Appl. Catal., A* **2008**, *338*, 52–57.

- (44) Liu, X.; Wang, A.; Yang, X.; Zhang, T.; Mou, C. Y.; Su, D. S.; Li, J. *Chem. Mater.* **2009**, *21*, 410–418.
- (45) Dekkers, M. A. P.; Lippits, M. J.; Nieuwenhuys, B. E. *Catal. Lett.* **1998**, *56*, 195–197.
- (46) Zanella, R.; Giorgio, S.; Henry, C. R.; Louis, C. J. *Phys. Chem. B* **2002**, *106*, 7634–7642.
- (47) Kresse, G.; Hafner, J. *Phys. Rev. B: Condens. Matter Mater. Phys.* **1993**, *47*, 558–561.
- (48) Kresse, G.; Furthmüller, J. *Comput. Mater. Sci.* **1996**, *6*, 15–50.
- (49) Hammer, B.; Hansen, L.; Nørskov, J. *Phys. Rev. B: Condens. Matter Mater. Phys.* **1999**, *59*, 7413–7421.
- (50) Almora-Barrios, N.; Carchini, G.; Błoński, P.; López, N. J. *Chem. Theory Comput.* **2014**, *10*, 5002–5009.
- (51) Kresse, G. *Phys. Rev. B: Condens. Matter Mater. Phys.* **1999**, *59*, 1758–1775.
- (52) Monkhorst, H. J.; Pack, J. D. *Phys. Rev. B* **1976**, *13*, 5188–5192.
- (53) Henkelman, G.; Uberuaga, B. P.; Jónsson, H. *J. Chem. Phys.* **2000**, *113*, 9901.
- (54) Shao, L.; Huang, X.; Teschner, D.; Zhang, W. *ACS Catal.* **2014**, *4*, 2369–2373.
- (55) Mitsudome, T.; Yamamoto, M.; Maeno, Z.; Mizugaki, T.; Jitsukawa, K.; Kaneda, K. *J. Am. Chem. Soc.* **2015**, *137*, 13452–13455.
- (56) Vasilikogiannaki, E.; Titilas, I.; Vassilikogiannakis, G.; Stratakis, M. *Chem. Commun.* **2015**, *51*, 2384–2387.
- (57) Li, S.-S.; Liu, X.; Liu, Y.-M.; He, H.-Y.; Fan, K.-N.; Cao, Y. *Chem. Commun.* **2014**, *50*, 5626–5628.
- (58) Liang, S.; Hammond, G. B.; Xu, B. *Chem. Commun.* **2016**, *52*, 6013–6016.
- (59) Jover, J.; García-Ratés, M.; López, N. *ACS Catal.* **2016**, *6*, 4135–4143.
- (60) Cano, I.; Huertos, M. a; Chapman, A. M.; Buntkowsky, G.; Gutmann, T.; Groszewicz, P. B.; van Leeuwen, P. W. N. *J. Am. Chem. Soc.* **2015**, *137*, 7718–7727.
- (61) Liu, C.; Abroshan, H.; Yan, C.; Li, G.; Haruta, M. *ACS Catal.* **2016**, *6*, 92–99.
- (62) Cano, I.; Chapman, A. M.; Urakawa, A.; van Leeuwen, P. W. N. *J. Am. Chem. Soc.* **2014**, *136*, 2520–2528.
- (63) López-Serrano, J.; Duckett, S. B.; Lledós, A. *J. Am. Chem. Soc.* **2006**, *128*, 9596–9597.
- (64) Chen, Z.; Pronkin, S.; Fellingner, T.-P.; Kailasam, K.; Vilé, G.; Albani, D.; Krumeich, F.; Leary, R.; Barnard, J.; Thomas, J. M.; Pérez-Ramírez, J.; Antonietti, M.; Dontsova, D. *ACS Nano* **2016**, *10*, 3166–3175.
- (65) Liu, P.; Zhao, Y.; Qin, R.; Mo, S.; Chen, G.; Gu, L.; Chevrier, D. M.; Zhang, P.; Guo, Q.; Zang, D.; Wu, B.; Fu, G.; Zheng, N. *Science* **2016**, *352*, 797–800.
- (66) Vilé, G.; Baudouin, D.; Remediakis, I. N.; Copéret, C.; López, N.; Pérez-Ramírez, J. *ChemCatChem* **2013**, *5*, 3750–3759.
- (67) Welch, G. C.; Juan, R. R. S.; Masuda, J. D.; Stephan, D. W. *Science* **2006**, *314*, 1124–1126.
- (68) Chernichenko, K.; Madarász, A.; Pápai, I.; Nieger, M.; Leskelä, M.; Repo, T. *Nat. Chem.* **2013**, *5*, 718–723.
- (69) Chorkendorff, I.; Niemantsverdriet, J. W. *Concepts of Modern Catalysis and Kinetics*; Wiley-VCH: Weinheim, FRG, 2003.
- (70) Carey, F. A.; Sundberg, R. J. *Advanced Organic Chemistry Part A: Structure and Mechanisms*; Springer: Boston, MA, USA, 2007.